

Dietary and Pharmacological Interventions That Inhibit Mammalian Target of Rapamycin Activity Alter the Brain Expression Levels of Neurogenic and Glial Markers in an Age- and Treatment-Dependent Manner

Dilan Celebi-Birand,^{1–3} Narin Ilgim Ardic,^{1–3} Elif Tugce Karoglu-Eravsar,^{1–3}
Goksemin Fatma Sengul,^{1–4} Hulusi Kafaligonul,^{1,3,5} and Michelle M. Adams^{1–3,6}

Abstract

Intermittent fasting (IF) and its mimetic, rapamycin extend lifespan and healthspan through mechanisms that are not fully understood. We investigated different short-term durations of IF and rapamycin on cellular and molecular changes in the brains of young (6–10 months) and old (26–31 months) zebrafish. Interestingly, our results showed that IF significantly lowered glucose levels while increasing DCAMKL1 in both young and old animals. This proliferative effect of IF was supported by the upregulation of *foxm1* transcript in old animals. Rapamycin did not change glucose levels in young and old animals but had differential effects depending on age. In young zebrafish, proliferating cell nuclear antigen and the LC3-II/LC3-I ratio was decreased, whereas glial fibrillary acidic protein and gephyrin were decreased in old animals. The changes in proliferative markers and a marker of autophagic flux suggest an age-dependent interplay between autophagy and cell proliferation. Additionally, changes in glia and inhibitory tone suggest a suppressive effect on neuroinflammation but may push the brain toward a more excitable state. Mammalian target of rapamycin (mTOR) activity in the brain following the IF and rapamycin treatment was differentially regulated by age. Interestingly, rapamycin inhibited mTOR more potently in young animals than IF. Principal component analysis supported our conclusion that the regulatory effects of IF and rapamycin were age-specific, since we observed different patterns in the expression levels and clustering of young and old animals. Taken together, our results suggest that even a short-term duration of IF and rapamycin have significant effects in the brain at young and old ages, and that these are age and treatment dependent.

Keywords: aging, brain, zebrafish, intermittent fasting, rapamycin, mTOR signaling

Introduction

LIFELONG CALORIC RESTRICTION (CR) and its mimetic, rapamycin, extend lifespan across species, improve health, and enhance cognitive abilities.^{1,2} Alterations in the brain underlying the beneficial effects of CR and rapamycin are becoming clear but questions remain about the timing and duration of diet and/or drug treatment.³ Furthermore, limited evidence exists on how exactly these variables affect presynaptic and postsynaptic components, cellular homeostasis, and neurogenesis.

Lifespan extension via CR or rapamycin involves mammalian target of rapamycin (mTOR)-dependent mecha-

nisms.⁴ mTOR is involved in cellular mechanisms including proliferation, autophagy, and survival.⁵ Homologs of mTOR have been identified in *Caenorhabditis elegans*,⁶ *Drosophila*,⁷ and zebrafish,⁸ indicating a conserved mechanism. The majority of studies have focused on the consequences of lifelong CR and most mimetics are chemical agents with side effects unsuitable for lifelong administration.⁹ Therefore, understanding of the outcomes of short-term CR/CR-mimetic applications is needed.

Presently, short-term durations of CR and rapamycin were tested using the zebrafish model organism. Zebrafish have recently emerged as a convenient model to study vertebrate aging.^{10,11} We applied alternate day feeding as an

¹Interdisciplinary Graduate Program in Neuroscience, Aysel Sabuncu Brain Research Center, Bilkent University, Ankara, Turkey.

²UNAM-Institute of Materials Science and Nanotechnology, Bilkent University, Ankara, Turkey.

³Zebrafish Facility, Bilkent University Molecular Biology and Genetics, Ankara, Turkey.

⁴Department of Cellular Biochemistry, Universitätsmedizin Göttingen, Göttingen, Germany.

⁵National Magnetic Resonance Research Center (UMRAM) and ⁶Department of Psychology, Bilkent University, Ankara, Turkey.

intermittent fasting (IF) regimen, which has been shown to share the same beneficial effects of CR.^{12,13}

Materials and Methods

Animal husbandry

Two-hundred seven wild-type (AB strain) zebrafish were used. One-hundred six animals were young (6–10 months old) and 101 were old (26–31 months old) with evenly distributed males and females. Fish were raised under standard conditions (27.5°C, 14L:10D cycle) being fed twice-a-day with fish flakes and once-a-day with 10 mg artemia in a recirculating system (Tecniplast, Italy). For IF and rapamycin treatment (RAPA), fish were grouped based on age and habituated under standard conditions in glass aquaria containing 4 L water. After 1 week, fish were randomly distributed into treatment groups and left to habituate 1 more week. Animals were fed *ad libitum* (AL) and weighed before treatment. The protocol for the experiments was in accordance with the international guidelines for the care and use of laboratory animals and approved by the Bilkent University Local Animal Ethics Committee with the following approval date and number: Feb 24, 2014 and 2014/11.

Feeding and drug treatment experiments

Throughout the 8-week experiment, fish were maintained under standard conditions. Feeding protocol was adapted from a previous study by our group.¹⁴ RAPA and AL animals were fed the same amounts (180 mg flakes twice-a-day, 10 mg artemia three times a week), while IF received 90 mg flakes twice-a-day every-other-day, and 10 mg artemia once a week. The protocol for RAPA was adapted from a previous study.¹⁵ Rapamycin (Sigma; R0395) was dissolved in dimethyl sulfoxide (DMSO) to reach 100 nM concentration and added into water in 1:1000 dilution. DMSO was added into water of AL and IF groups. Since rapamycin's half-life is 62 ± 16 hours,⁹ three-quarters of the water was replaced with fresh system water once every 3 days. Both the pH and nitrate levels were periodically measured. To prevent stocking-related stress, the number of fish per tank was set to a maximum density of 5 fish/L, consistent with the literature.^{16–18} At the end of 4, 6, and 8 weeks, animals were euthanized in ice water. Final body weight and length were measured. Brains and trunks were immediately snap-frozen and preserved at -80°C . Samples were processed separately to quantify individual differences.

Whole-body glucose measurements

A novel method was developed in guidance of previous studies^{19,20} to measure whole-body glucose concentration. Frozen fish trunks were homogenized in 2 mL ice-cold $1 \times$ Dulbecco's phosphate buffer saline. Homogenates were centrifuged at 5000 rpm for 5 minutes at room temperature. Ten microliters of supernatant was used for glucose measurement with a Bayer Contour Plus Glucometer.

Western blot

Protein isolation from brain tissues and western blots were performed as previously described.²¹ Individual brain protein samples were loaded onto a 5–10/13% resolving gel under denaturing conditions. Each sample was run at least three times being systematically rotated in the gel. Details about the anti-

bodies are provided in Supplementary Table 1. Signal detection was done with SuperSignalTM Femto (Thermo Fisher Scientific) in ChemiDocTM XRS+ (BioRad). Band densities were quantified using ImageJ software (NIH) by N.I.A., an author in this study blinded as to the sample source for an unbiased analysis. The data were double-normalized as described previously.²² We first normalized each value to the intensity of 4-week AL in each gel (*i.e.*, within-gel normalization). Next, within-gel-normalized values for each sample were divided by the within-gel-normalized values of the housekeeping protein β -tubulin of the corresponding sample (*i.e.*, tubulin normalization).

Total RNA isolation, DNase treatment, and cDNA synthesis

Total RNA was isolated from fish brains with the TRIzol reagent (Thermo Fisher Scientific) following the manufacturer's instructions. Individual brains were homogenized in 400 μL TRIzol using a 26-gauge, 1 mL syringe. RNA concentration was measured using NanoDropTM 2000 (Thermo Fisher Scientific). RNA samples were treated with TURBO DNA-freeTM Kit (Thermo Fisher Scientific), and cDNAs were synthesized from 500 ng/ μL of DNase-treated samples with the iScriptTM cDNA Synthesis Kit (Bio-Rad).

Gene expression analysis by quantitative reverse transcription PCR

Reactions were done in 20 μL volume, using 2 μL cDNA, 5 μM of each forward and reverse primers (Supplementary Table 2), and LightCycler[®] 480 SYBR Green I Master (Roche, Switzerland). The primer pairs targeting each gene of interest being *foxm1*,²³ *atg5*, and *lc3b*²⁴ previously validated in zebrafish, and *igf1* primers designed by us.²⁵ The PCRs were carried out in a LightCycler 480 instrument. Relative expression levels of each gene of interest to β -actin were calculated using the $2^{-\Delta\text{CT}}$. The fold change was calculated using the $2^{-\Delta\Delta\text{CT}}$ method, by normalizing to the average relative expression of all samples followed by Log₂ transformation. A heatmap of fold change values was generated using the Heatmapper tool.²⁶

Statistical analysis

Statistical analysis was performed using the SPSS software (IBM). Analysis of variance (ANOVA) was done for each factor when assumptions of normal distribution and homogeneity of variances were validated via Kolmogorov–Smirnov and Levene's tests. Two-way and three-way ANOVAs were utilized to determine overall effects and *post hoc* analyses were carried out using Bonferroni correction. Simple effects analyses were performed to dissect possible interactions between factors. A Kruskal–Wallis test followed by Mann–Whitney *U* test for pairwise comparisons was employed for instances when the two assumptions were violated. Significance levels were set at $p < 0.05$ unless corrected and more stringent for multiple comparisons. In all cases duration effects were analyzed separately and together, allowing for increased statistical power for any age and treatment effects. Situations where duration effects were significant were reported separately.

Principal component analysis (PCA) was performed by using SPSS software. Components were extracted based on eigenvalues set above the 0.5 level. Kaiser–Meyer–Olkin

Measure of Sampling Adequacy (KMO) and Bartlett's Test of Sphericity were conducted to validate the efficiency of dimension reduction. Components were rotated by using the Varimax with Kaiser normalization method.

Results

IF but not RAPA decreased body weight, mass index, and glucose

Results demonstrated that both age and treatment had an overall effect on body weight ($F_{(1,208)}=89.299$ and $F_{(2,208)}=$

18.969; $p \leq 0.001$, respectively), body mass index (BMI) ($F_{(1,206)}=12.917$ and $F_{(2,206)}=25.329$; $p \leq 0.001$, respectively), and whole-body glucose levels ($\chi^2_{(1)}=9.859$ and $\chi^2_{(2)}=13.851$; $p \leq 0.002$, respectively). Mean weight and BMI of young and old IF animals were lower (Fig. 1a–d; $p \leq 0.05$) than *ad libitum* (AL)-fed counterparts after 8 weeks of IF. Different patterns of body weight changes were observed within the young and old AL and IF groups. The young AL (Y-AL) group gained weight, from 4 to 8 weeks (Fig. 1a; $p \leq 0.01$), whereas old AL (O-AL) animals showed no change in body weight (Fig. 1b). However, there was a decrease in BMI and body weight in old IF (O-IF)

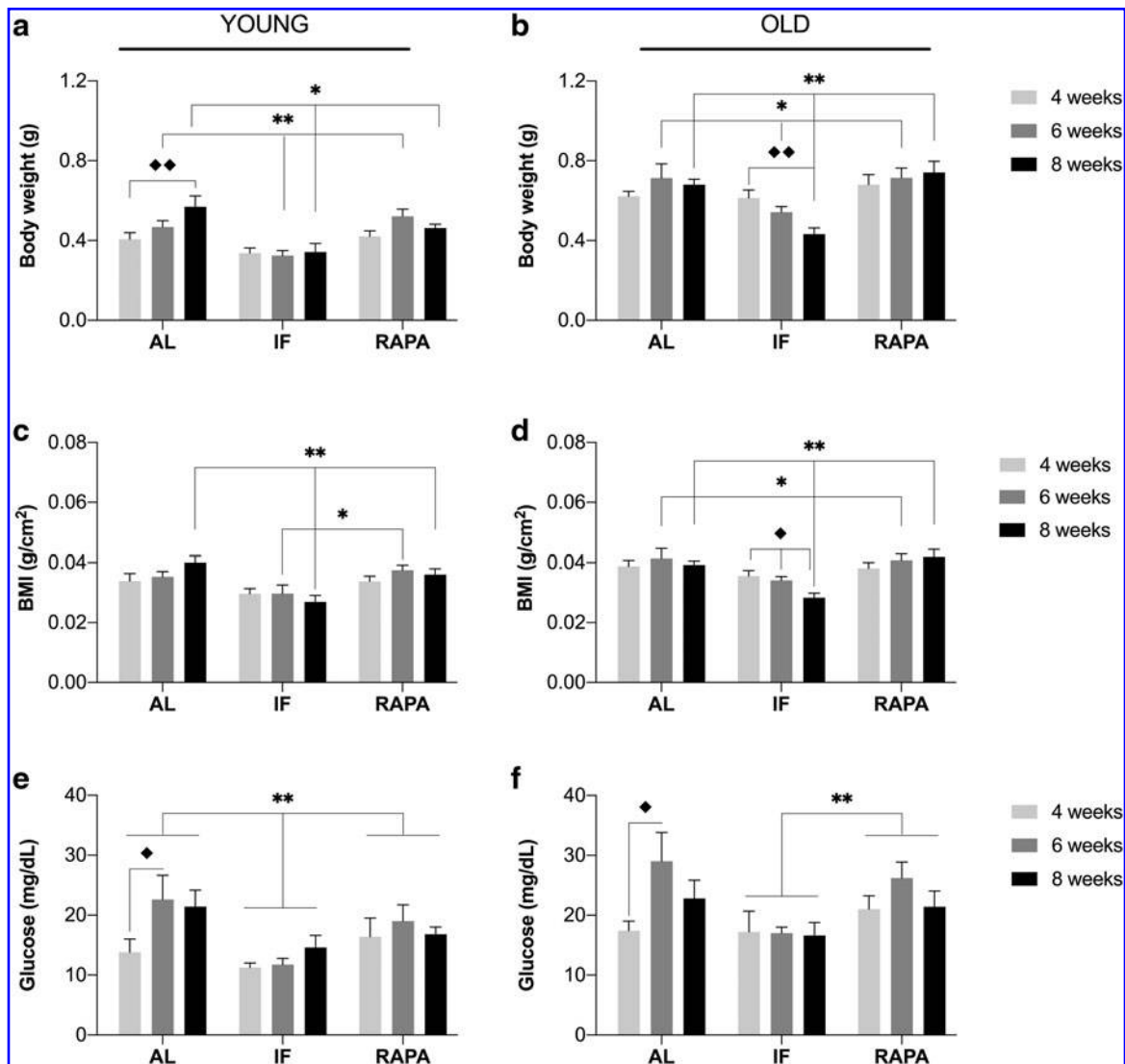


FIG. 1. Changes in body weight, BMI, and glucose in response to different durations of intermittent fasting and rapamycin treatment in young (a, c, e) and old animals (b, d, f). The results demonstrated that both age and treatment had an overall significant effect on body weight ($F_{(1,208)}=89.299$ and $F_{(2,208)}=18.969$; $p \leq 0.001$, respectively), BMI ($F_{(1,206)}=12.917$ and $F_{(2,206)}=25.329$; $p \leq 0.001$, respectively), and whole-body glucose levels ($\chi^2_{(1)}=9.859$ and $\chi^2_{(2)}=13.851$; $p \leq 0.002$, respectively). There was a significant interaction between treatment and duration for both body weight and BMI ($F_{(4,208)}=3.512$; $p \leq 0.01$ and $F_{(4,206)}=2.845$; $p \leq 0.05$, respectively). There was a marginally significant effect of duration on glucose ($\chi^2_{(2)}=5.946$; $p=0.051$). Both Y-IF and O-IF had a significantly lower body weight (a, b) and BMI (c, d) than AL-fed counterparts by the end of 8 weeks. O-IF animals experienced a significant decrease in body weight (b) and BMI (d). IF significantly reduced whole-body glucose levels in both young (e) and old animals (f). Group means at a given duration are shown, and the error bar represents one standard error (SE). BMI is calculated from the body weight and length measurements at the end of each dietary period. AL, *ad libitum*-fed control group; IF, intermittent fasting group; RAPA, rapamycin-treated group. Diamond (◆) represents within group differences (◆◆ $p \leq 0.01$, ◆ $p \leq 0.05$), and asterisk (*) represents across group differences (** $p \leq 0.01$, * $p \leq 0.05$). For weight and BMI measurements, $N=10-14$. For glucose measurements, $N=4-6$. BMI, body mass index.

between 4 and 8 weeks (both p -values ≤ 0.05), while no changes were observed in young IF (Y-IF) (Fig. 1c, d). Data demonstrated no differences in body weight or BMI between RAPA-treated and AL-fed animals for both ages, indicating that the drug itself did not adversely affect these variables. Consistent with the literature, whole-body glucose levels were lower in both Y-IF and O-IF groups when compared to AL-fed counterparts²⁷ (Fig. 1e, f; $p \leq 0.01$). Finally, glucose levels were higher in O-IF and O-RAPA animals than in Y-IF and Y-RAPA (both p -values ≤ 0.02), confirming an age-related increase in glucose levels.²⁸

Short-term durations of IF and RAPA suppressed mTOR activity

To investigate short-term effects of IF and RAPA on mTOR activity in the young and old brains, we first determined whether IF and RAPA altered phospho-mTOR (p-mTOR^{Ser2481}) levels. Ser2481 residue of mTOR is an autophosphorylation site, and mTOR Ser(P) -2481 is inhibited by rapamycin treatment.²⁹ We observed a treatment effect on p-mTOR^{Ser2481} in young animals ($\chi^2_{(2)} = 11.808$, $p = 0.003$), but not in old (Fig. 2a), with lower phosphoprotein levels in Y-IF and Y-RAPA compared to Y-AL ($p \leq 0.004$). We quantified total and phospho-4E-BP1 (p-4E-BP1), a downstream target of mTOR.³⁰ There were no effects on total 4E-BP1 (Fig. 2b) but treatment affected p-4E-BP1 levels (Fig. 2c; $\chi^2_{(2)} = 14.664$, $p = 0.001$) and the ratio of p-4E-BP1/4E-BP1 (Fig. 2d; $\chi^2_{(2)} = 7.674$, $p = 0.022$) differentially in young and old fish. RAPA decreased p-4E-BP1 and p-4E-BP1/4E-BP1 levels in young but not in old animals (Fig. 2c,d, respectively, $p \leq 0.001$). IF did not show anything significant. These results indicate that short-term RAPA has a stronger inhibitory effect on mTOR activity in young animals, supporting age-specific modulation of mTOR function. Protein bands were observed at the expected size (Fig. 2e).

RAPA downregulated gephyrin, while age affected PSD-95 and synaptophysin levels

We investigated how presynaptic and postsynaptic markers changed in response to IF and RAPA. We quantified PSD-95 and GEP as postsynaptic markers of excitatory and inhibitory synapses, respectively (Fig. 3a, b).³¹ There was an effect of age on PSD-95 ($\chi^2_{(1)} = 9.181$, $p = 0.002$) with PSD-95 expression levels being lower in Y-RAPA than O-RAPA ($p = 0.012$). GEP was affected by treatment but only in old animals ($\chi^2_{(2)} = 6.870$, $p = 0.032$), with a decrease between O-IF and O-RAPA ($p = 0.011$), indicating that IF modulates GEP levels in old animals. Duration also affected GEP levels in O-RAPA with longer duration lowering their expression (Supplementary Fig. 1a; $\chi^2_{(2)} = 7.485$, $p = 0.024$).

To determine whether there may be a change in the excitatory/inhibitory (E/I) balance, we compared the PSD-95/GEP ratio across groups since alterations in this has been recognized as an essential component of neural plasticity, and affected by both age³² and diet-induced shifts in brain energy metabolism.³³ Our data demonstrated a treatment effect on PSD-95/GEP levels (Fig. 3c; $\chi^2_{(2)} = 7.694$, $p = 0.021$). The age effect was limited to the RAPA group with O-RAPA having a higher E/I ratio than Y-RAPA ($\chi^2_{(1)} = 6.193$, $p = 0.013$).

How IF and RAPA modulate the presynaptic compartment was examined by quantifying expression levels of SYP and LC3. SYP is a presynaptic vesicle protein³⁴ altered with age.^{35,36} LC3 is involved in autophagy, a mechanism implicated in synaptic homeostasis and modulated by RAPA.³⁷ LC3 exists in two forms: LC3-I is the cytosolic form, needing to be lipidated (LC3-II) for recruitment to autophagosomes.³⁷ Therefore, both LC3-II and LC3-II/LC3-I were quantified to assess autophagic flux. Age significantly affected SYP (Fig. 3d; $\chi^2_{(1)} = 5.108$, $p = 0.024$) and is consistent with older animals having higher basal levels.³⁸ O-AL fish had higher SYP levels than Y-AL (Fig. 3d; $p = 0.055$). No changes in LC3-I (Fig. 3e) and LC3-II (Fig. 3f) occurred, however, treatment affected LC3-II/LC3-I (Fig. 3g; $\chi^2_{(2)} = 8.518$, $p = 0.014$) with this ratio being reduced in Y-RAPA ($p = 0.005$) and O-IF groups ($p = 0.023$). Age also affected the ratio of LC3-II/LC3-I (Fig. 3g; $\chi^2_{(1)} = 7.376$, $p = 0.007$) with it being higher in O-AL and O-RAPA animals than their young counterparts ($p \leq 0.02$).

IF upregulated DCAMKL1 while RAPA downregulated proliferating cell nuclear antigen and glial fibrillary acidic protein

We investigated whether proliferative markers were altered by IF and RAPA in the brain. We quantified the global proliferation marker, proliferating cell nuclear antigen (PCNA),³⁹ neural progenitor cell marker, DCAMKL1,⁴⁰ and activated astrocyte marker, glial fibrillary acidic protein (GFAP).⁴¹ Treatment and age had effects on PCNA levels (Fig. 3h; $\chi^2_{(2)} = 6.665$, $p = 0.036$ and $\chi^2_{(1)} = 3.930$, $p = 0.047$, respectively). While treatment effects on DCAMKL1 levels were in young and old fish (Fig. 3i; $\chi^2_{(2)} = 13.100$, $p = 0.001$), they only occurred in old animals for GFAP (Fig. 3j; $\chi^2_{(2)} = 9.084$, $p = 0.011$). PCNA expression decreased in Y-RAPA compared with Y-AL (Fig. 3g; $p = 0.002$) and O-RAPA (Fig. 3g; $p = 0.026$). DCAMKL1 expression levels increased in Y-IF and O-IF compared with their AL counterparts (Fig. 3i; $p \leq 0.02$). Finally, GFAP levels decreased in O-RAPA as compared with O-AL and O-IF (Fig. 3h; $p = 0.006$). These results suggest that these treatments differentially affect neuronal and astrocytic proliferative capacity in an age-specific manner. Protein bands were observed at the expected size (Fig. 3k).

Genes involved in proliferation were altered age specifically while autophagy genes were not affected by age and treatment

Expression levels of the following genes were measured: Forkhead Box M1 (*foxm1*), implicated in proliferation; insulin-like growth factor 1 (*igf1*) in nutrient signaling; autophagy-related 5 (*atg5*) and LC3 Beta (*lc3b*), which are required for autophagic cascades. Both *foxm1* and *igf1* are involved in lifespan regulation and *igf1* is direct target of *foxm1*.⁴² Data demonstrated effects of treatment on *foxm1* in old animals with O-IF and O-RAPA having higher levels than O-AL (Fig. 4a; $\chi^2_{(2)} = 8.226$, $p = 0.016$; O-AL–O-IF, $p = 0.030$). Treatment decreased *igf1* expression levels in Y-RAPA animals compared with age-matched counterparts (Fig. 4b; $\chi^2_{(2)} = 7.250$, $p = 0.027$). Downregulation of *igf1* in young animals in response to mTOR inhibition is consistent with the literature,⁴³ while the upregulation of *foxm1* in old

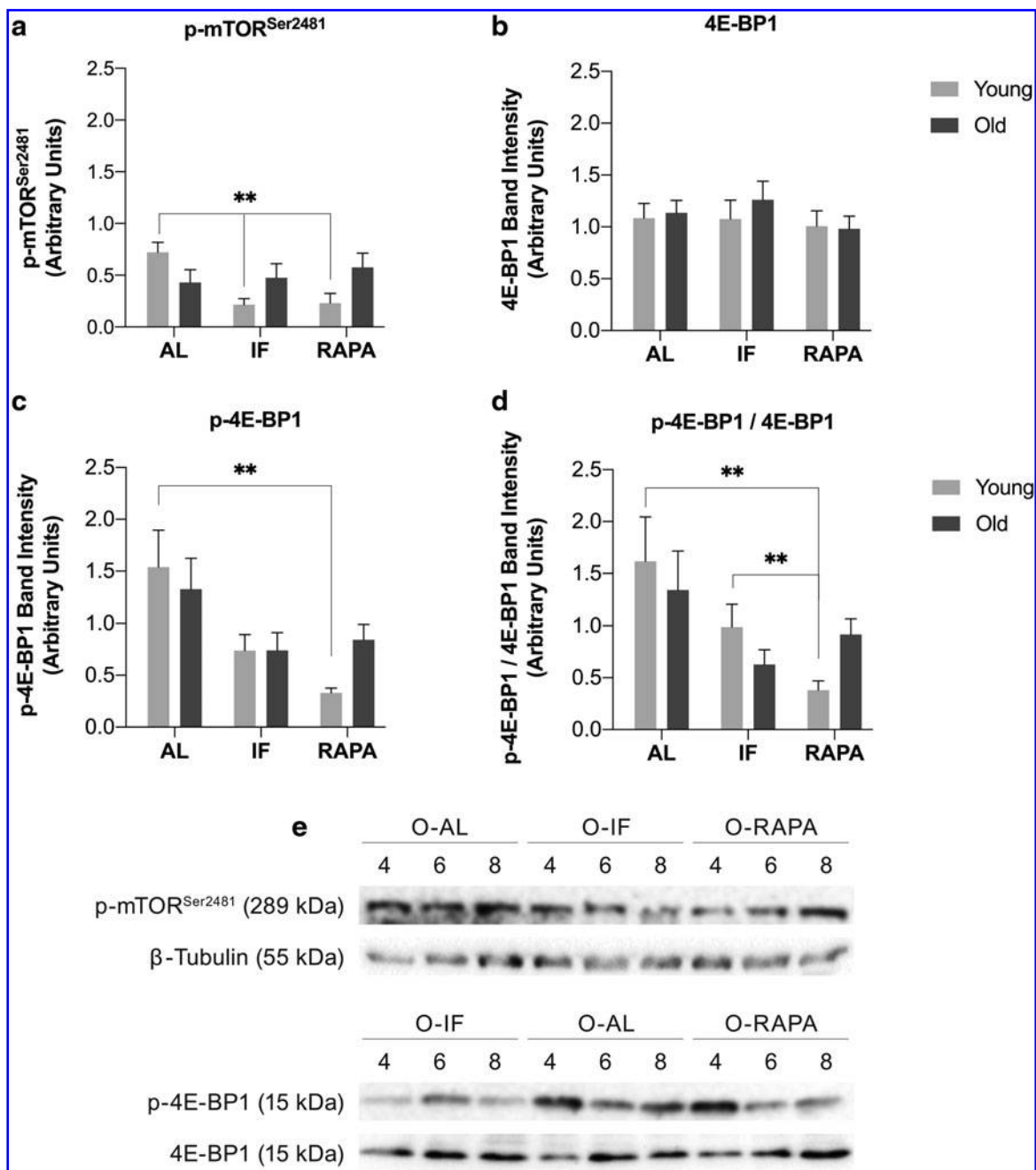


FIG. 2. Changes in the expression levels of p-mTOR^{Ser2481} (a), 4E-BP1 (b), p-4E-BP1 (c), and the ratio of p-4E-BP1/4E-BP1 (d) in response to RAPA or IF in young and old animals. Representative blots showed the expected bands at ~289 kDa corresponding to p-mTOR^{Ser2481}, 15 kDa corresponding to 4E-BP1 and its phosphorylated version p-4E-BP1, and β -tubulin at 55 kDa (e). The bands represent one individual western blot experiment from one individual old brain of one technical replicate. Treatment significantly affected p-mTOR^{Ser2481} levels in young animals ($\chi^2_{(2)} = 11.808$, $p = 0.003$), and p-4E-BP1 and p-4E-BP1/4E-BP1 in both age groups ($\chi^2_{(2)} = 14.664$, $p = 0.001$ and $\chi^2_{(2)} = 7.674$, $p = 0.022$, respectively). Rapamycin significantly reduced p-mTOR^{Ser2481} (a), p-4E-BP1 (c), p-4E-BP1/4E-BP1 (d) with no differences in 4E-BP1 levels in young animals (b). The p-mTOR^{Ser2481} expression was also reduced in Y-IF (a). Group means obtained from band intensities in arbitrary units are shown as bars, and the error bar represents one standard error (SE). The data from three durations are combined for each group. $N = 9-14$ for all groups. $**p \leq 0.01$. mTOR, mammalian target of rapamycin.

animals is novel. Taken together, these results suggest a differential response in young and old to reduced mTOR activity.

To determine whether autophagy was induced in brains of young and old zebrafish, we quantified the mRNA

transcripts of two autophagy-related genes: *atg5* and *lc3b*. There were no effects of age and treatment on *atg5* and *lc3b* levels (Fig. 4c, d). Duration affected *lc3b* expression levels (Supplementary Fig. 1b, c; $\chi^2_{(2)} = 10.067$, $p = 0.007$).

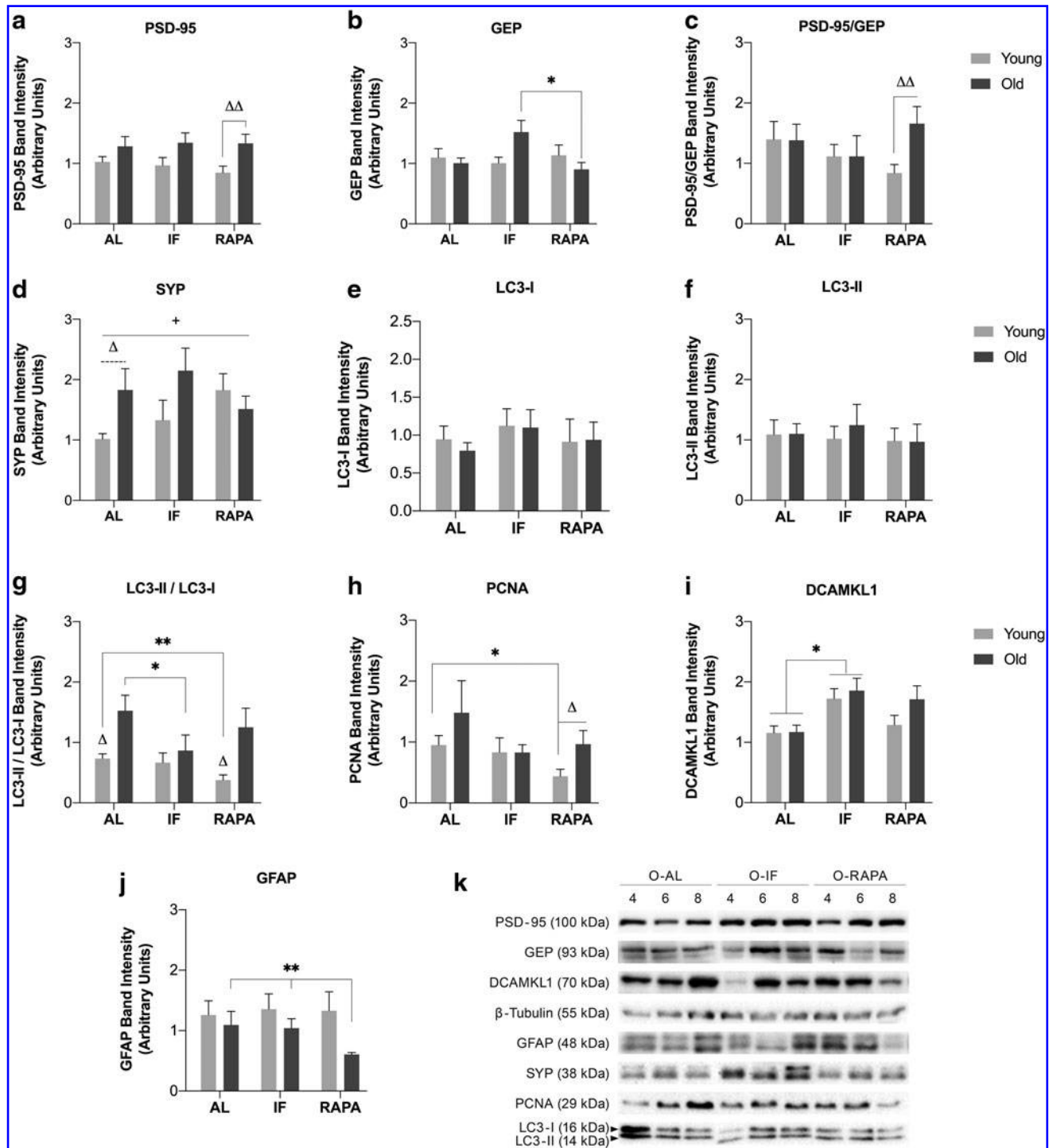


FIG. 3. Changes in the expression levels of PSD-95 (a), GEP (b), the ratio of PSD-95/GEP (c), SYP (d), LC3-I (e), LC3-II (f), LC3-II/LC3-I (g), PCNA (h), DCAMKL1 (i), and GFAP (j) in response to RAPA treatment or IF in young and old animals. Representative blots showed the expected bands at ~100 kDa for PSD-95, 93 kDa for GEP, 70 kDa for DCAMKL1, 55 kDa for β -tubulin, 48 kDa for GFAP, 38 kDa for SYP, 29 kDa for PCNA, 16 kDa for LC3-I, and 14 kDa for LC3-II (k). The bands represent one individual western blot experiment from one individual old brain of one technical replicate. Significant age effects were observed in PSD-95 ($\chi^2_{(1)}=9.181$, $p=0.002$; a), PSD-95/GEP ($\chi^2_{(1)}=6.193$, $p=0.013$; c), SYP ($\chi^2_{(1)}=5.108$, $p=0.024$; d), LC3-II/LC3-I ($\chi^2_{(1)}=7.376$, $p=0.007$; g), and PCNA ($\chi^2_{(1)}=3.930$, $p=0.047$, h). IF significantly increased GEP in old animals (b). Diet and drug treatment decreased LC3-II/LC3-I levels in an age-dependent manner (g). RAPA downregulated PCNA (h) in young animals, and GFAP in old animals (j). DCAMKL1 was upregulated by IF in both age groups (i). Group means obtained from band intensities in arbitrary units are shown as bars, and the error bar represents one standard error (SE). Asterisk (*) represents across group differences (** $p \leq 0.01$, * $p \leq 0.05$), plus sign (+) represents significant age effect (+ $p \leq 0.05$), and triangle (Δ) represents age differences ($\Delta\Delta p \leq 0.01$, $\Delta p \leq 0.05$). The dashed line represents marginally significant changes ($p \leq 0.06$). The data from three durations are combined for each group. $N=6-15$ for PCNA, $N=9-14$ for LC3-II, and LC3-II/LC3-I, and $N=11-16$ for the rest of the quantifications.

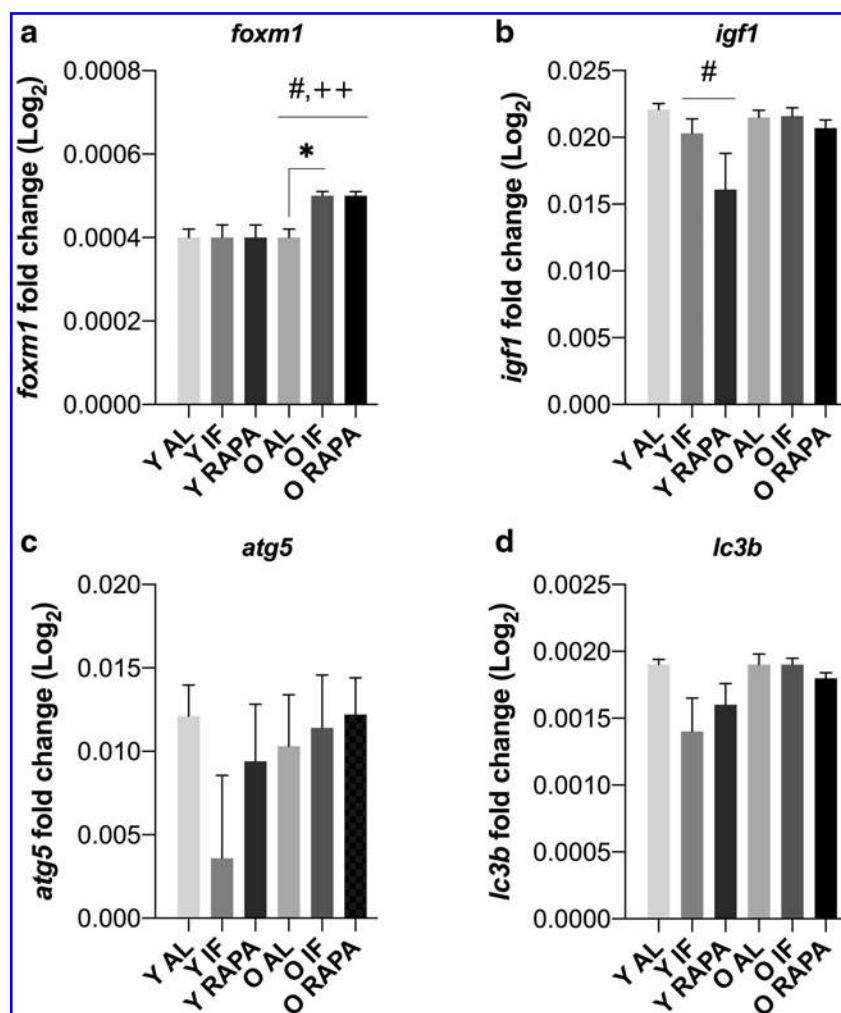


FIG. 4. Log₂-fold changes in the expression levels of *foxm1* (a), *igf1* (b), *atg5* (c), and *lc3b* (d) genes in young and old IF and RAPA animals. The *foxm1* transcript was significantly affected by age and treatment, and IF upregulated *foxm1* expression in old animals (a). A significant treatment effect was observed in the expression levels of *igf1* (b). Y, young; O, old. * $p \leq 0.05$, hashtags (#) and plus signs (++) represent significant treatment ($p \leq 0.05$) and age ($p \leq 0.01$) effects, respectively. The data from three durations are combined for each group. $N = 11-15$ for all groups.

PCA of proteins of interest revealed differential clustering patterns in young and old animals in response to IF and RAPA

PCA was performed on the significantly affected proteins of interest to investigate how each factor correlates with one another across different age and treatment groups. Three components were extracted and validated with Bartlett's and KMO tests. The Bartlett's test determined that correlations in the correlation matrix were significant ($\chi^2_{(55)} = 126.490$, $p < 0.001$), and a strong relationship between variables were observed (KMO = 0.471). Eigenvalues and explained variance of each component, and items with component loading scores above 0.40 are given in Table 1. In the first principal component (PC1), GFAP was the factor with the highest loading score, in PC2, it was p-4E-BP1 and p-4E-BP1/4E-BP1, and in PC3, it was PSD-95/GEP.

All of the significant correlations from the output of the PCA are reported in Table 2. The most notable and novel is that p-4E-BP1 was negatively correlated with DCAMKL1, suggesting a suppressive effect of mTOR activity on neu-

rogenesis. Interestingly, p-mTOR^{Ser2481} was positively correlated with PCNA, GFAP, and PSD-95, indicating a role in inducing proliferation, neuroinflammation, and excitatory neurotransmission. Finally, positive correlations were observed between p-mTOR^{Ser2481} and p-4E-BP1, confirming the expected regulatory effect of mTOR on 4E-BP1. For data visualization, components obtained from PCA were saved as variables and each sample was displayed in a matrix of scatterplots (Fig. 5). In IF and AL, the clusters formed by young and old animals were closer compared to distinct clusters in RAPA. This indicates a more uniform expression pattern in IF and AL across lifespan, while RAPA clearly acted in an age-dependent manner.

Discussion

Currently, how factors such as age of subjects and duration of IF or RAPA contribute to their healthspan-extending effects in the brain were examined. We utilized young and old zebrafish, and analyzed their response to varying durations of IF

TABLE 1. EIGENVALUES AND EXPLAINED VARIANCES FOR EACH COMPONENT IN THE PRINCIPAL COMPONENT ANALYSIS, AND FACTORS WITH HIGHEST LOADING SCORES IN EACH COMPONENT

		<i>Eigenvalue</i>	<i>Explained variance (%)</i>	<i>Component loading scores (>0.4)</i>				
Principal Component (Protein expression data)	1	2.680	24.36	GFAP (0.85)	PCNA (0.744)	p-mTOR (0.709)	PSD-95 (0.62)	LC3-II/LC3-I (0.479)
	2	2.386	21.69	p-4E-BP1/4E-BP1 (0.894)	p-4E-BP1 (0.894)	DCAMKL1 (−0.684)		
	3	1.505	13.68	PSD-95/GEP (0.921)	GEP (−0.739)	PSD-95 (0.473)		

The eigenvalues and explained variances are obtained from PCA by using IBM SPSS software. The factors with the loading scores of 0.4 and above in each principal component are shown. The factors with the highest loading scores are highlighted in gray.

DCAMKL1, doublecortin-like kinase 1; GEP, gephyrin; GFAP, glial fibrillary acidic protein; PCA, principal component analysis; PCNA, proliferating cell nuclear antigen; PSD-95, postsynaptic density-95.

and RAPA to evaluate its potential efficacy as an IF-mimetic. Results demonstrated age-specific responses to IF and RAPA treatment, mainly independent of duration. Moreover, these effects were prominent from whole body, that is, BMI and glucose, to brain, that is, alterations at the cellular and molecular level (Fig. 6).

Data showed that young animals were more resistant to diet-induced weight loss than old. This suggests a minimum BMI at both ages is needed to maintain a healthy state since O-IF and Y-IF reached a similar level by 8 weeks. Mean weight of Y-AL animals increased significantly while there were no changes in that of O-AL. Zebrafish grow continuously into adulthood, and this phase extends beyond the age of 6 months,⁴⁴ which we used for initiation of the treatments in young adult subjects. This growth pattern could explain why young and old zebrafish are affected differentially by diet. Finally, RAPA treatment did not affect body weight or BMI suggesting fish did not suffer any adverse effects of the drug.

Young and old animals subjected to IF or RAPA could have differences in metabolic parameters such as total glucose levels. Since glucose is the main energy source of the brain and alters protein levels,⁴⁵ it is an important parameter to examine in response to age and treatment. Whole-body glucose levels were significantly lower in Y-IF and O-IF compared with AL-fed counterparts (Fig. 6), validating this dietary regimen to regulate glucose metabolism.²⁷ Lack of such observations in RAPA groups (Fig. 6) might indicate a mild glucose intolerance previously reported in response to RAPA.⁴⁶ Since differences in plasma glucose levels reflect those in the central nervous system,⁴⁷ any changes likely contribute to those observed in cellular and molecular markers but in an age-dependent manner.

Short-term IF caused lower body glucose levels in both young and old zebrafish. While they both had lower glucose, the pattern of cellular responses in the brain, although somewhat similar, was age dependent. Y-IF and O-IF groups demonstrated increases in levels of DCAMKL1, a neuronal marker, but the cellular responses depended on the animal's age (Fig. 6). In the Y-IF group, glucose and p-mTOR^{Ser2481} levels were decreased in parallel with increases in DCAMKL1. Whereas in the O-IF group, glucose levels were lower but with decreases in the autophagic flux marker, the LC3-II/LC3-I ratio, and increases not only in DCAMKL1 but also the more general proliferative marker, *foxm1*. Its protein product, FOXM1, a transcription factor regulating adult neurogenesis, is expressed in GFAP⁺ im-

mature precursors and DCAMKL1⁺ NPCs.⁴⁰ Studies across lifespan demonstrated lower proliferation rates⁴⁸ and neurogenesis in brains of older animals.⁴⁹ This could be partially explained by decreases in *foxm1* expression levels during aging.⁵⁰ The direction of the effects between these markers is well-established and consistent with the literature.^{51–53} Overall these data suggest while short-term IF decreases glucose and increases expression of neurogenic markers in young and old animals there appear to be different cellular mechanisms depending on subject's age. Further studies need to examine whether the changes in cellular and neuronal proliferation marker protein levels correspond to differences in total cell numbers. This could be done by counting double-labeled bromodeoxyuridine cells with different cell-specific lineage markers. Data from our group demonstrated that 10 weeks of IF does not alter the course of age-related alterations in numbers of proliferating cells.¹⁴ Therefore, those results along with the current ones indicate IF effects are limited to subtle changes within cells.

Unlike short-term IF, treatment with the IF-mimetic, rapamycin, resulted in no changes in body glucose levels in young and old zebrafish, likely representing a mild glucose intolerance. In addition, while Y-RAPA and O-RAPA animals showed stable glucose levels, the brain cellular and molecular responses were entirely different across ages (Fig. 6). In the Y-RAPA group, *igf1* and p-mTOR^{Ser2481} decreased, along with p-4E-BP1 and the p-4E-BP1/4E-BP1 ratio. There were overall decreases in the autophagic flux marker, the LC3-II/LC3-I ratio, and global cell proliferation marker, PCNA. These data suggest that in Y-RAPA, decreases in levels of autophagy may be protecting the pool of NPCs. Autophagy either leads to survival or apoptosis depending on the state of the cell.⁵⁴ The patterns observed in Y-RAPA of decreases in PCNA expression indicate that this treatment may control proliferation by regulating autophagic cascades. Autophagy has been shown to be essential for CR to extend lifespan,⁵⁵ and neuroprotection by rapamycin treatment.⁵⁶ However, there are contradicting results such as upregulation of *atg5* and *lc3b* in response to CR and RAPA,^{57,58} or CR-mediated downregulation of *lc3b* and LC3B-II/LC3B-I in young animals.⁵⁹ This indicates that our data would be in agreement with the literature. Unlike young animals, the O-RAPA-treated fish showed no changes in global proliferation. However, there were alterations in neuronal and glial markers with decreases in GFAP and GEP expression levels and no changes in PSD-95. GFAP is a marker of immature

TABLE 2. CORRELATION COEFFICIENTS AND THE SIGNIFICANCE OF CORRELATIONS BETWEEN THE PROTEINS OF INTEREST

Correlation	PSD-95	SYP	GEP	PSD-95/GEP	DCAMKL1	p-4E-BP1	GFAP	p-4E-BP1/4E-BP1	PCNA	p-mTOR	LC3-II/LC3-I
PSD-95	1	0.219	0.115	0.612	-0.072	-0.097	0.399	-0.069	0.126	0.432	0.221
SYP	0.219	1	-0.003	0.031	-0.142	-0.041	0.078	-0.006	0.272	0.016	0.1
GEP	0.115	-0.003	1	-0.561	-0.183	0.081	0.184	0.041	-0.03	0.299	-0.113
PSD-95/GEP	0.612	0.031	-0.561	1	0.097	-0.177	0.13	-0.127	-0.005	0.137	0.147
DCAMKL1	-0.072	-0.142	-0.183	0.097	1	-0.423	0.174	-0.392	0.011	-0.15	0.166
p-4E-BP1	-0.097	-0.041	0.081	-0.177	-0.423	1	0.112	0.822	0.197	0.357	-0.081
GFAP	0.399	0.078	0.184	0.13	0.112	0.822	1	0.009	0.719	0.445	0.215
p-4E-BP1/4E-BP1	-0.069	-0.006	0.041	-0.127	-0.392	0.009	0.033	1	0.033	0.267	-0.105
PCNA	0.126	0.272	-0.03	-0.005	0.011	0.197	0.719	0.033	1	0.373	0.245
p-mTOR	0.432	0.016	0.299	0.137	-0.15	0.357	0.445	0.267	0.373	1	0.291
LC3-II/LC3-I	0.221	0.1	-0.113	0.147	0.166	-0.081	0.215	-0.105	0.245	0.291	1
Sig. (1- tailed)											
PSD-95	0.132	0.132	0.281	0	0.358	0.311	0.018	0.363	0.261	0.011	0.13
SYP	0.281	0.495	0.495	0.437	0.236	0.417	0.347	0.487	0.081	0.468	0.307
GEP	0	0.437	0.001	0.001	0.175	0.342	0.174	0.418	0.44	0.061	0.284
PSD-95/GEP	0.358	0.236	0.001	0.312	0.312	0.184	0.255	0.26	0.489	0.244	0.227
DCAMKL1	0.311	0.417	0.342	0.184	0.012	0.012	0.187	0.019	0.479	0.223	0.2
p-4E-BP1	0.018	0.347	0.174	0.255	0.187	0.285	0	0	0.158	0.031	0.34
GFAP	0.018	0.347	0.174	0.255	0.187	0.285	0.481	0.481	0	0.009	0.135
p-4E-BP1/4E-BP1	0.363	0.487	0.418	0.26	0.019	0	0	0.434	0.434	0.085	0.298
PCNA	0.261	0.081	0.44	0.489	0.479	0.158	0	0.085	0.025	0.025	0.105
p-mTOR	0.011	0.468	0.061	0.244	0.223	0.031	0.009	0.298	0.025	0.066	0.066
LC3-II/LC3-I	0.13	0.307	0.284	0.227	0.2	0.34	0.135	0.298	0.105	0.066	0.066

The correlation coefficients (upper panel) and significance levels (lower panel) for the proteins of interest are given in the table. Strong (upper panel) and significant correlations (lower panel) are indicated in dark gray.

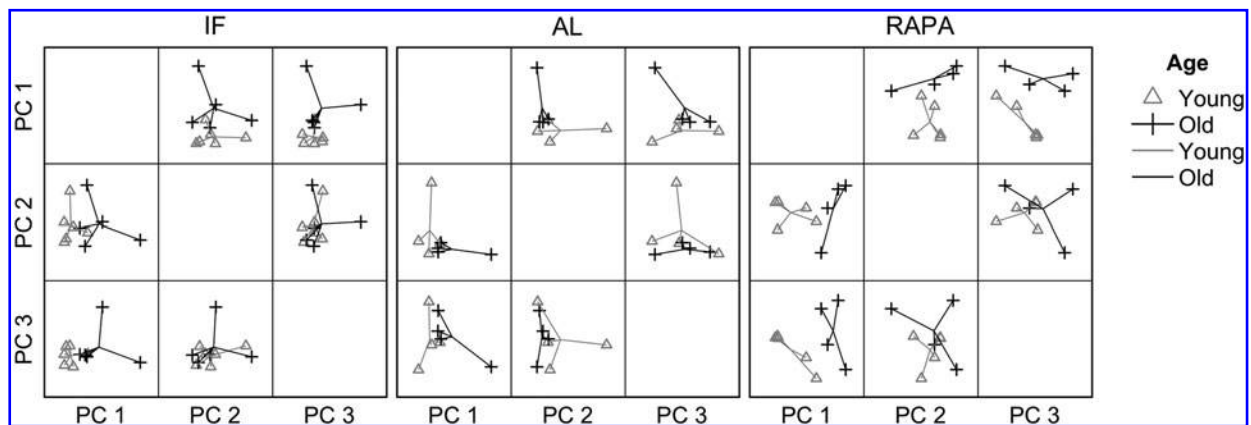


FIG. 5. Expression levels of proteins of interest cluster in an age- and treatment-specific manner in the principal component matrices. On the PC1 axis, in which GFAP is the strongest contributor, young animals were clustered closer to the lower margin. This suggests reduced neuroinflammation in young animals compared with old animals. Y-IF and Y-RAPA clusters were located on lower margin of the PC2 axis, in which p-4E-BP1 had the strongest contribution. This indicates a suppression of mTOR activity through both interventions. On the PC3 axis, PSD-95/GEP-driven clustering suggested that IF regulated the E/I ratio similarly across lifespan whereas RAPA had age-dependent effects.

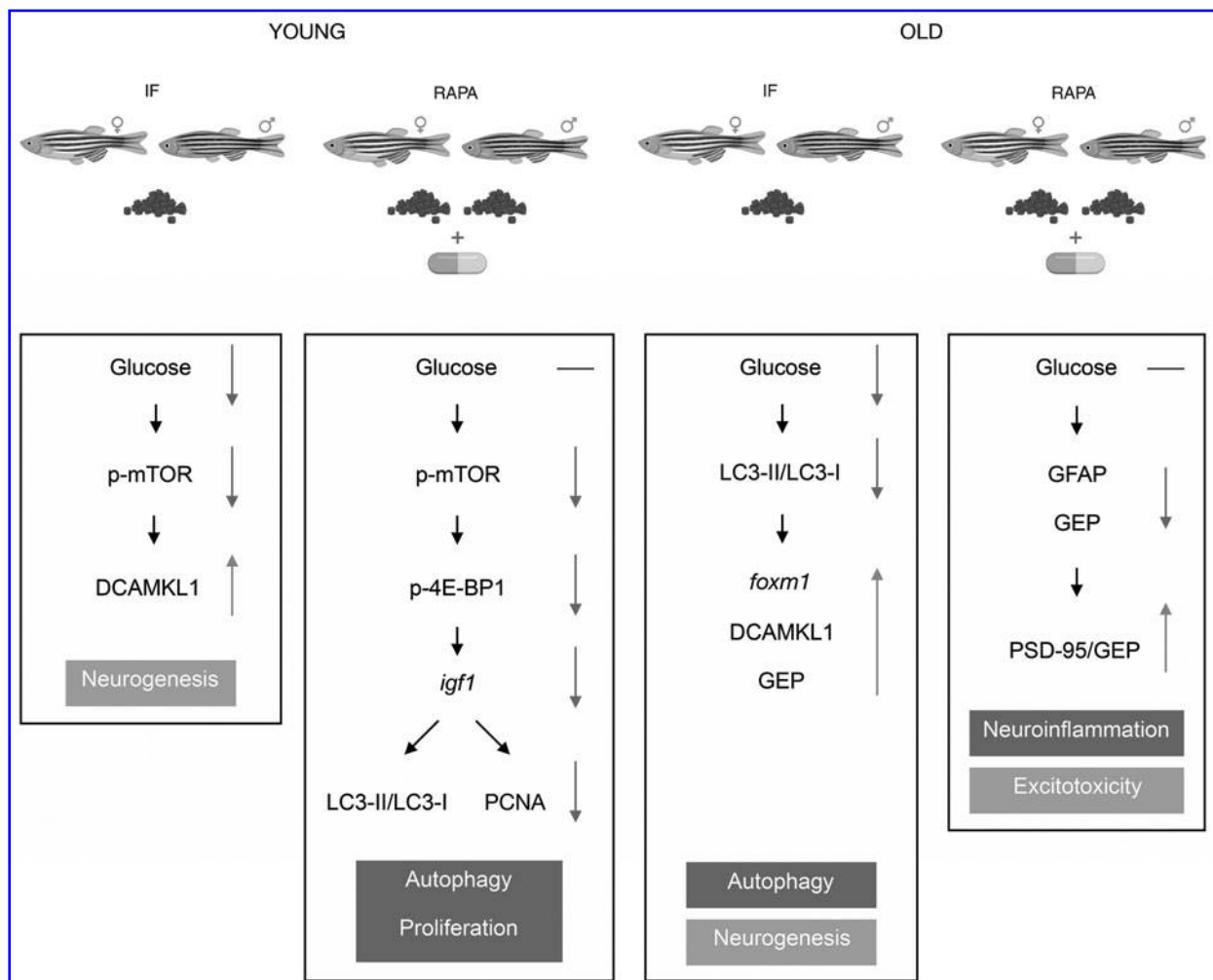


FIG. 6. Summary figure depicting the age-related changes in response to IF and RAPA in young and old animals. IF decreased whole-body glucose and mTOR phosphorylation levels, which promoted upregulation of neural progenitor marker DCAMKL1 in young animals. In old animals, IF decreased glucose and LC3-II/LC3-I while increasing GEP, *foxm1*, and DCAMKL1. These suggested a common response to IF in young and old animals, but through distinct molecular mechanisms. RAPA did not alter glucose levels yet was able to decrease p-mTOR and p-4E-BP1 in young animals. Both overall proliferation and autophagic flux were suppressed in Y-RAPA. In old animals, RAPA decreased GEP and GFAP levels, suggesting a restriction on the inhibitory tone and neuroinflammation. Upward and downward arrows indicate upregulation and downregulation, respectively. Dashes represent no observed difference. The molecular mechanisms that have been upregulated are represented with light gray boxes, and downregulated processes are shown in dark gray boxes. The figure was created with BioRender.

precursors that give rise to DCAMKL1-expressing NPCs, and activated astrocytes involved in an inflammatory response able to be reduced by rapamycin treatment.⁴¹ Concomitant decreases in GEP and GFAP expression with no changes in PSD-95 would likely reduce the possibility of increased neuroinflammation⁶⁰ but move the brain toward a more excitable state possibly promoting cellular excitotoxicity.⁶¹

The hypothesis of the brain being in a more excited state is additionally supported by our data revealing the O-RAPA group has a higher PSD-95/GEP ratio, or E/I balance. It is well established that RAPA can directly regulate GFAP levels⁴¹ but these data show a novel finding of controlling GEP expression levels. To our knowledge, this is the first report on RAPA-induced downregulation of GEP. The inhibitory marker, GEP, forms clusters on postsynaptic sites through mTOR-dependent mechanisms⁶² and this downregulation is likely due to inhibition of cluster formation and increased availability of free GEP targeted for degradation.⁶³ Future studies should be directed at closely analyzing the role of rapamycin-induced downregulation of GEP, and to why PSD-95, a marker of excitatory synapses, is protected.

Quantification of phosphoproteins confirmed that RAPA and to a lesser extent, IF, inhibit mTOR activity in the brain in an age-dependent manner. RAPA reduced phosphorylation levels of mTOR and 4E-BP1 in young fish, but not old animals. The age-dependent lack of inhibition of p-mTOR^{Ser2481} may occur because mTOR exists in two complexes: mTOR complex 1 (mTORC1) and 2 (mTORC2). p-mTOR^{Ser2481} has been observed in both complexes, yet RAPA is known to inhibit p-mTOR^{Ser2481} more effectively in mTORC1.²⁹ Since mTORC2 activity increases with age, it might compensate for decreased mTORC1 activity in old animals.⁶⁴ Future studies examining IF-mimetic effects across lifespan need to be directed toward varying drug concentrations according to subjects' age for precise mTOR inhibition.

To achieve a complete understanding of how different components modulating synaptic transmission are affected by IF and RAPA, we quantified SYP, a presynaptic marker of synaptic integrity and function. SYP expression levels were higher in old animals when compared to young, and there was an increase in O-AL compared with Y-AL fish. Our results demonstrating higher levels of SYP in old subjects and no significant effects of mTOR inhibition on presynaptic components are consistent with the literature.^{35,65} Indeed, the distinct functions of mTORC1 and mTORC2 in the postsynaptic and presynaptic sites, respectively, have been reported.⁶⁶

To conclude, our results indicate age-specific responses to IF and RAPA treatment. Both IF and RAPA altered glucose levels similarly in young and old animals. However, the cellular and molecular responses were similar between IF-fed young and old animals but dissimilar between young and old RAPA-treated fish. These data suggest that response to diet and its mimetics is age and treatment dependent and this should be taken into account with regard to any potential translation to human subjects.

Acknowledgement

Authors would like to thank Tulay Arayici for excellent technical assistance with animal experiments, and B. Simay Uner for help with experiments.

Authors' Contribution

D.C.B. performed experiments and helped writing the article, N.I.A. assisted with dissections and feedings, and quantifying western blot data, E.T.K.E. with statistical analysis and data interpretation, G.F.S. with feedings and dissections, H.K. with funding support and critically reading the article, and M.M.A. conceived the experimental design, as well as doing results interpretation, article preparation, and securing funding. All approved the final version of the article.

Author Disclosure Statement

No competing financial interests exist.

Funding Information

This work was supported by The Scientific and Technological Research Council of Turkey (TUBITAK), Ankara, Turkey [grant number 214S236].

Supplementary Material

Supplementary Table S1
Supplementary Table S2
Supplementary Figure S1

References

1. Chung KW, Kim DH, Park MH, et al. Recent advances in calorie restriction research on aging. *Exp Gerontol* 2013; 48:1049–1053.
2. Wahl D, Cogger VC, Solon-Biet SM, et al. Nutritional strategies to optimise cognitive function in the aging brain. *Ageing Res Rev* 2016;31:80–92.
3. Picó C, Palou M, Priego T, Sánchez J, Palou A. Metabolic programming of obesity by energy restriction during the perinatal period: Different outcomes depending on gender and period, type and severity of restriction. *Front Physiol* 2012;3:1–14.
4. Saxton RA, Sabatini DM. mTOR Signaling in Growth, Metabolism, and Disease. *Cell* 2017;168:960–976.
5. Laplante M, Sabatini DM. Regulation of mTORC1 and its impact on gene expression at a glance. *J Cell Sci* 2013; 126(Pt 8):1713–1719.
6. Long X, Spycher C, Han ZS, Rose AM, Müller F, Avruch J. TOR deficiency in *C. elegans* causes developmental arrest and intestinal atrophy by inhibition of mRNA translation. *Curr Biol* 2002;12:1448–1461.
7. Oldham S. Genetic and biochemical characterization of dTOR, the *Drosophila* homolog of the target of rapamycin. *Genes Dev* 2000;14:2689–2694.
8. Makky K, Tekiela J, Mayer AN. Target of rapamycin (TOR) signaling controls epithelial morphogenesis in the vertebrate intestine. *Dev Biol* 2007;303:501–513.
9. FDA. RAPAMUNE (sirolimus) ORAL SOLUTION AND TABLETS. 1999:1–46. www.accessdata.fda.gov/drugsatfda_docs/label/2010/021110s0581bl.pdf.
10. Kishi S, Uchiyama J, Baughman AM, Goto T, Lin MC, Tsai SB. The zebrafish as a vertebrate model of functional aging and very gradual senescence. *Exp Gerontol* 2003;38: 777–786.
11. Adams MM, Kafaligonul H. Zebrafish—a model organism for studying the neurobiological mechanisms underlying cognitive brain aging and use of potential interventions. *Front Cell Dev Biol* 2018;6:1–5.

12. Mattson MP, Wan R. Beneficial effects of intermittent fasting and caloric restriction on the cardiovascular and cerebrovascular systems. *J Nutr Biochem* 2005;16:129–137.
13. Martin B, Mattson MP, Maudsley S. Caloric restriction and intermittent fasting: Two potential diets for successful brain aging. *Ageing Res Rev* 2006;5:332–353.
14. Arslan-Ergul A, Erbab A, Karoglu ET, Halim DO, Adams MM. Short-term dietary restriction in old zebrafish changes cell senescence mechanisms. *Neuroscience* 2016;334:64–75.
15. Goldsmith MI, Iovine MK, O'Reilly-Pol T, Johnson SL. A developmental transition in growth control during zebrafish caudal fin development. *Dev Biol* 2006;296:450–457.
16. Pavlidis M, Digka N, Theodoridi A, et al. Husbandry of Zebrafish, *Danio rerio*, and the cortisol stress response. *Zebrafish* 2013;10:524–531.
17. Matthews M, Trevarrow B, Matthews J. A virtual tour of the Guide for zebrafish users. *Lab Anim (NY)* 2002;31:34–40.
18. Lidster K, Readman GD, Prescott MJ, Owen SF. International survey on the use and welfare of zebrafish *Danio rerio* in research. *J Fish Biol* 2017;90:1891–1905.
19. Eames SC, Philipson LH, Prince VE, Kinkel MD. Blood sugar measurement in zebrafish reveals dynamics of glucose homeostasis. *Zebrafish* 2010;7:205–213.
20. Römisch-Margl W, Prehn C, Bogumil R, Röhring C, Suhre K, Adamski J. Procedure for tissue sample preparation and metabolite extraction for high-throughput targeted metabolomics. *Metabolomics* 2012;8:133–142.
21. Karoglu ET, Halim DO, Erkaya B, et al. Aging alters the molecular dynamics of synapses in a sexually dimorphic pattern in zebrafish (*Danio rerio*). *Neurobiol Aging* 2017;54:10–21.
22. Adams MM, Shi L, Linville MC, et al. Caloric restriction and age affect synaptic proteins in hippocampal CA3 and spatial learning ability. *Exp Neurol* 2008;211:141–149.
23. Sucularli C, Shehwana H, Kuscü C, Dungul DC, Ozdag H, Konu O. Functionally conserved effects of rapamycin exposure on zebrafish. *Mol Med Rep* 2016;13:4421–4430.
24. Meng XH, Chen B, Zhang JP. Intracellular insulin and impaired autophagy in a zebrafish model and a cell model of type 2 diabetes. *Int J Biol Sci* 2017;13:985–995.
25. Arslan-Ergul A, Adams MM. Gene expression changes in aging Zebrafish (*Danio rerio*) brains are sexually dimorphic. *BMC Neurosci* 2014;15:29.
26. Babicki S, Arndt D, Marcu A, et al. Heatmapper: web-enabled heat mapping for all. *Nucleic Acids Res* 2016;44:W147–W153.
27. Cho Y, Hong N, Kim K, et al. The effectiveness of intermittent fasting to reduce body mass index and glucose metabolism: A systematic review and meta-analysis. *J Clin Med* 2019;8:1645.
28. O'Sullivan JB. Age gradient in blood glucose levels: Magnitude and clinical implications. *Diabetes* 1974;23:713–715.
29. Soliman GA, Acosta-Jaquez HA, Dunlop EA, et al. mTOR Ser-2481 autophosphorylation monitors mTORC-specific catalytic activity and clarifies rapamycin mechanism of action. *J Biol Chem* 2010;285:7866–7879.
30. Fingar DC, Salama S, Tsou C, Harlow E, Blenis J. Mammalian cell size is controlled by mTOR and its downstream targets S6K1 and 4EBP1/eIF4E. *Genes Dev* 2002;16:1472–1487.
31. Micheva KD, Busse B, Weiler NC, O'Rourke N, Smith SJ. Single-synapse analysis of a diverse synapse population: Proteomic imaging methods and markers. *Neuron* 2010;68:639–653.
32. Peinemann A, Lehner C, Conrad B, Siebner HR. Age-related decrease in paired-pulse intracortical inhibition in the human primary motor cortex. *Neurosci Lett* 2001;313:33–36.
33. Greene AE, Todorova MT, Seyfried TN. Perspectives on the metabolic management of epilepsy through dietary reduction of glucose and elevation of ketone bodies. *J Neurochem* 2003;86:529–537.
34. Valtorta F, Pennuto M, Bonanomi D, Benfenati F. Synaptophysin: Leading actor or walk-on role in synaptic vesicle exocytosis? *BioEssays* 2004;26:445–453.
35. Ando S, Tanaka Y, Toyoda Y, Kon K, Kawashima SI. Turnover of synaptic membranes: Age-related changes and modulation by dietary restriction. *J Neurosci Res* 2002;70:290–297.
36. Park SW, Lee JG, Seo MK, et al. Differential effects of antidepressant drugs on mTOR signalling in rat hippocampal neurons. *Int J Neuropsychopharmacol* 2014;17:1831–1846.
37. Vijayan V, Verstreken P. Autophagy in the presynaptic compartment in health and disease. *J Cell Biol* 2017;216:1895–1906.
38. Eastwood SL, Weickert CS, Webster MJ, Herman MM, Kleinman JE, Harrison PJ. Synaptophysin protein and mRNA expression in the human hippocampal formation from birth to old age. *Hippocampus* 2006;16:645–654.
39. Moldovan GL, Pfander B, Jentsch S. PCNA, the maestro of the replication fork. *Cell* 2007;129:665–679.
40. Genin EC, Caron N, Vandenbosch R, Nguyen L, Malgrange B. Concise review: Forkhead pathway in the control of adult neurogenesis. *Stem Cells* 2014;1398–1407.
41. Goldshmit Y, Kanner S, Zacs M, et al. Rapamycin increases neuronal survival, reduces inflammation and astrocyte proliferation after spinal cord injury. *Mol Cell Neurosci* 2015;68:82–91.
42. Sengupta A, Kalinichenko VV, Yutzey KE. FoxO1 and FoxM1 transcription factors have antagonistic functions in neonatal cardiomyocyte cell-cycle withdrawal and IGF1 gene regulation. *Circ Res* 2013;112:267–277.
43. Sonntag WE, Lenham JE, Ingram RL. Effects of Aging and Dietary Restriction on Tissue Protein Synthesis: Relationship to Plasma Insulin-like Growth Factor-1. *J Gerontol* 1992;47:B159–B163.
44. Singleman C, Holtzman NG. Growth and maturation in the zebrafish, *Danio rerio*: A staging tool for teaching and research. *Zebrafish* 2014;11:396–406.
45. Mergenthaler P, Lindauer U, Dienel GA, Meisel A. Sugar for the brain: The role of glucose in physiological and pathological brain function. *Trends Neurosci* 2013;36:587–597.
46. Yu Z, Wang R, Fok WC, Coles A, Salmon AB, Pérez VI. Rapamycin and dietary restriction induce metabolically distinctive changes in mouse liver. *J Gerontol Ser A Biol Sci Med Sci* 2015;70:410–420.
47. Gruetter R, Ugurbil K, Seaquist ER. Steady-state cerebral glucose concentrations and transport in the human brain. *J Neurochem* 2002;70:397–408.
48. Heine VM, Maslam S, Joëls M, Lucassen PJ. Prominent decline of newborn cell proliferation, differentiation, and apoptosis in the aging dentate gyrus, in absence of an age-related hypothalamus-pituitary-adrenal axis activation. *Neurobiol Aging* 2004;25:361–375.

49. Kuhn HG, Dickinson-Anson H, Gage FH. Neurogenesis in the dentate gyrus of the adult rat: age-related decrease of neuronal progenitor proliferation. *J Neurosci* 1996;16: 2027–2033.
50. Vaughan S, Jat PS. Deciphering the role of nuclear factor- κ B in cellular senescence. *Aging* (Albany NY) 2011;3: 913–919.
51. Fusco S, Leone L, Barbati SA, et al. A CREB-Sirt1-Hes1 circuitry mediates neural stem cell response to glucose availability. *Cell Rep* 2016;14:1195–1205.
52. Sato A, Sunayama J, Matsuda K ichiro, et al. Regulation of neural stem/progenitor cell maintenance by PI3K and mTOR. *Neurosci Lett* 2010;470:115–120.
53. Ramírez-Peinado S, León-Annicchiarico CL, Galindo-Moreno J, et al. Glucose-starved cells do not engage in prosurvival autophagy. *J Biol Chem* 2013;288:30387–30398.
54. White E, DiPaola RS. The double-edged sword of autophagy modulation in cancer. *Clin Cancer Res* 2009;15:5308–5316.
55. Blagosklonny M V. Linking calorie restriction to longevity through sirtuins and autophagy: Any role for TOR. *Cell Death Dis* 2010;1:e12–e13.
56. Pan T, Rawal P, Wu Y, Xie W, Jankovic J, Le W. Rapamycin protects against rotenone-induced apoptosis through autophagy induction. *Neuroscience* 2009;164: 541–551.
57. Mercken EM, Crosby SD, Lamming DW, et al. Calorie restriction in humans inhibits the PI3K/AKT pathway and induces a younger transcription profile. *Aging Cell* 2013; 12:645–651.
58. Lee SE, Kim EY, Choi HY, et al. Rapamycin rescues the poor developmental capacity of aged porcine oocytes. *Asian-Australas J Anim Sci* 2014;27:635–647.
59. Sheng Y, Lv S, Huang M, et al. Opposing effects on cardiac function by calorie restriction in different-aged mice. *Aging Cell* 2017;16:1155–1167.
60. Brahmachari S, Fung YK, Pahan K. Induction of glial fibrillary acidic protein expression in astrocytes by nitric oxide. *J Neurosci* 2006;26:4930–4939.
61. Agarwal S, Tannenberg RK, Dodd PR. Reduced expression of the inhibitory synapse scaffolding protein gephyrin in Alzheimer's disease. *J Alzheimer's Dis* 2008;14:313–321.
62. Wuchter J, Beuter S, Treindl F, et al. A Comprehensive small interfering RNA screen identifies signaling pathways required for gephyrin clustering. *J Neurosci* 2012;32: 14821–14834.
63. Tyagarajan SK, Ghosh H, Yévenes GE, et al. Regulation of GABAergic synapse formation and plasticity by GSK3 β -dependent phosphorylation of gephyrin. *Proc Natl Acad Sci U S A* 2011;108:379–384.
64. Chellappa K, Brinkman JA, Mukherjee S, et al. Hypothalamic mTORC2 is essential for metabolic health and longevity. *Aging Cell* 2019;18:e13014.
65. Niere F, Raab-Graham KF. mTORC1 is a local, postsynaptic voltage sensor regulated by positive and negative feedback pathways. *Front Cell Neurosci* 2017;11:152.
66. McCabe MP, Cullen ER, Barrows CM, et al. Genetic inactivation of mTORC1 or mTORC2 in neurons reveals distinct functions in glutamatergic synaptic transmission. *Elife* 2020;9:e51440.

Address correspondence to:

Michelle M. Adams

Interdisciplinary Graduate Program in Neuroscience

Aysel Sabuncu Brain Research Center

Bilkent University

Ankara 06800

Turkey

E-mail: michelle@bilkent.edu.tr

Received: December 25, 2019

Accepted: April 10, 2020